Transport of continental air to the subantarctic Indian Ocean

Yves Balkanski, Daniel J. Jacob

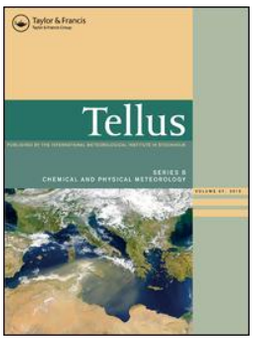

Tellus B: Chemical and Physical Meteorology

ISSN: (Print) 1600-0889 (Online) Journal homepage: https://www.tandfonline.com/loi/zelb20

Transport of continental air to the subantarctic Indian Ocean

Yves J. Balkanski & Daniel J. Jacob

To cite this article: Yves J. Balkanski & Daniel J. Jacob (1990) Transport of continental air to the subantarctic Indian Ocean, Tellus B: Chemical and Physical Meteorology, 42:1, 62-75, DOI: 10.3402/tellusb.v42i1.15192

To link to this article: https://doi.org/10.3402/tellusb.v42i1.15192

Published online: 18 Jan 2017.

Tellus (1990), *42B*, 62–75

Transport of continental air to the subantarctic Indian Ocean

By YVES J. BALKANSKI and DANIEL J. JACOB, *Department of Earth & Planetary Sciences and Division of Applied Sciences, Pierce Hall, 29 Oxford St., Harvard University, Cambridge, Massachusetts 02138, USA*

(Manuscript received 24 January 1989; in final form 17 August 1989)

ABSTRACT

The occurrence of high levels of atmospheric ^{222}Rn (radonic storms) at 3 subantarctic islands in the Indian Ocean is simulated with a 3-d chemical tracer model (CTM) based on the meteorology of the GISS general circulation model (GCM). Radon-222 (half-life 3.8 days) is a sensitive tracer of continental air over the oceans. The CTM simulates well the observed intensities of the radonic storms at the islands, their seasonal frequency (highest in winter), and their periodicity (25–28 days). The storms are due to fast boundary layer advection of air from South Africa, made possible by the conjunction of a subtropical high SE of Madagascar (Mascarene High) and a mid-latitudes low off the southern tip of the African continent. Transit times of air from South Africa to the islands range from 1 to 5 days. The Mascarene high is a semi-permanent feature of the circulation from May to October, and is responsible for the seasonal frequency of the radonic storms. The low is transient but exhibits an oscillation of period 23–28 days which appears to be responsible for the observed periodicity of the storms. Transport to the subantarctic Indian Ocean is the principal mechanism for ventilation of South Africa in the CTM, but most of this transport takes place in the free troposphere following deep convection over the continent. The boundary layer advection mechanism associated with radonic storms accounts for only a small fraction of the total continental air exported to the subantarctic Indian Ocean.

1. Introduction

This paper attempts to explain the occurrence of high ^{222}Rn episodes (radonic storms) observed at 3 islands in the subantarctic Indian Ocean (Fig. 1): Crozet (51°52′E, 46°26′S), Kerguelen (70°15′E, 49°21′S), Amsterdam (77°34′E, 37°50′S). Radon-222 is a radioisotope (half-life 3.8 days) produced by decay of ^{226}Ra from crustal material. Emission rates from oceans are at least 2 orders of magnitude lower than from land (Broecker et al., 1967; Wilkening and Clements, 1975). 20-year records of ^{222}Rn concentrations are available from the 3 islands, which are located 2800 km (Crozet), 4200 km (Kerguelen), and 5000 km (Amsterdam) off the African coast (Lambert et al., 1970; Polian et al.,

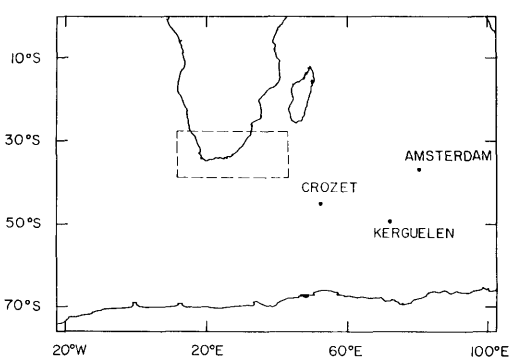

Fig. 1. Detail of the region under study indicating the 3 island sites in the Indian Ocean (Crozet, Kerguelen, Amsterdam). The dashed line indicates the boundaries of the South Africa airshed defined in Section 5.

1986). Baseline concentrations at the islands are of order 1 pCi/SCM; by comparison, surface concentrations over continents are typically 100–400 pCi/SCM (Lambert et al., 1982; Gesell, 1983). The baselines are disturbed occasionally by episodes in which ^{222}Rn concentrations rise abruptly to 5–40 pCi/SCM and remain elevated for time intervals ranging from several hours to a few days. These radonic storms cannot usually be accounted for by local ^{222}Rn emissions from the islands (Lambert et al., 1970; Polian et al., 1986) and are instead the signature of rapid transport of continental air over the ocean. We simulate here the occurrence of radonic storms with a 3-d chemical tracer model (CTM) based on the meteorology from a general circulation model (GCM) developed at the Goddard Institute of Space Studies (GISS). The origin of the storms will be examined in light of the CTM results and with the assistance of meteorological observations.

Long-range transport of continental air over the oceans has been documented in several field studies (Carlson and Prospero, 1972, Uematsu et al., 1983; Merrill et al., 1985; Polian et al., 1986; Whelpdale et al., 1988; Andreae et al., 1988; Lenschow et al., 1988), and has been confirmed by satellite observations (Fishman et al., 1989). This transport is thought to take place mainly in the free troposphere, following deep convection over the continents; the continental air is eventually brought to the surface of the ocean by subsidence (Merrill et al., 1985; Newell et al., 1988; Kritz et al., 1990) or by precipitation scavenging (Whelpdale et al., 1988). Concentrations of ^{222}Rn over the oceans are usually higher in the free troposphere than in the boundary layer, in accord with such a mechanism for transport (Polian et al., 1986; Lenschow et al., 1988). However, as pointed out by Polian et al. (1986), the sharp episodic nature of the radonic storms observed over the subantarctic Indian Ocean, and the low dilution factors compared to ^{222}Rn mixing ratios over continents, argue for a more direct continental origin. We will show below that the vast majority of these radonic storms can be explained by rapid boundary layer advection of air from southern Africa.

The radonic storms at Crozet and Kerguelen exhibit a remarkable periodicity of 27–28 days (Lambert et al., 1970). A similar periodicity (25–30 days) has been reported for radonic storms at Commandante Ferraz on King George Island, located near the Antarctic Peninsula 1000 km off the tip of South America (Pereira, 1990). Meteorological oscillations with period 20–30 days are well-known features of the monsoonal circulation over the tropical Indian Ocean (Krishnamurti and Bhalme, 1976; Cadet, 1983), of the zonal wind at southern mid-latitudes (Kidson, 1986), and of lower stratospheric waves in the southern hemisphere (Leovy and Webster, 1976), but it is unclear whether these oscillations can explain the periodicity of the radonic storms. To date there have been no studies specific to the subantarctic Indian Ocean. Lambert et al. (1970) suggested that the 28-day periodicity in the intensity of corpuscular radiation from the sun could lead to a global meteorological oscillation with the same periodicity, but they did not elaborate. We will argue below that the observed periodicity of the radonic storms in the subantarctic Indian Ocean is caused by the oscillation of a transient mid-latitudes low off the southern tip of Africa. This oscillation appears to be simulated by the GCM, which restricts speculation as to its possible origin.

Rapid export of air from South Africa to the subantarctic Indian Ocean, as documented by the observation of radonic storms, could constitute a major source of pollution to southern mid-latitudes. South Africa is an industrial country which emits large amounts of pollutants from fossil fuel combustion (Fuggle and Rabie, 1983). The atmosphere at southern mid-latitudes is generally regarded as defining background tropospheric conditions, with minimum perturbation from anthropogenic influences (Fraser et al., 1986). The good simulation of radonic storms by the CTM suggests that the model describes accurately at least one mechanism for pollutant transport from South Africa to southern mid-latitudes. Further analysis of the CTM data provides insights into other transport mechanisms and the associated mass fluxes. We will see that the boundary layer advection mechanism associated with radonic storms accounts for only a minor fraction of the total continental air exported from South Africa to the subantarctic Indian Ocean. Most of this transport takes place in the free troposphere.

The CTM used in the present study has been

applied previously with success to the simulation of several long-lived tracers including CO_2 (Fung et al., 1983), CFC's (Prather et al., 1987) and ^{85}Kr (Jacob et al., 1987). In these previous studies, the CTM was operated on a $8° \times 10°$ spatial grid, with 8-h time steps; we adopt here a finer resolution which accommodates the relatively short half-life of ^{222}Rn and which resolves the detail of air trajectories from the African continent to the subantarctic islands. A summary description of the CTM is given in Section 2. The simulated time series of ^{222}Rn concentrations at the 3 islands are compared to observations in Section 3. The origin of ^{222}Rn storms is investigated in Section 4. The seasonal frequencies and the periodicities of the storms are examined in Section 5, and implications for transport of continental air to the subantarctic Indian Ocean are discussed.

2. Model description

The CTM solves the 3-d continuity equation for the concentration of ^{222}Rn on a $4° \times 5°$ grid with 9 layers in the vertical, following the grid of the $4° \times 5°$ GISS GCM II (Hansen et al., 1983). The vertical layers are defined using sigma coordinates (Hansen et al., 1983), and the 3 lowest layers extend to approximately 500, 1200, and 2600 m above ground. The CTM domain includes the entire atmosphere up to 10 mb in order to avoid errors from boundary conditions. Transport is computed over 4-h time steps and includes separate contributions from advection, convection (both wet and dry), and turbulent diffusion, as discussed in detail by Prather et al. (1987) and Jacob and Prather (1990). First- and second-order moments of ^{222}Rn concentration are conserved at all steps of the computation, so that the concentration within a gridbox is described by a 2nd-order polynomial in 3 dimensions (Prather, 1986). The meteorological input to the CTM simulation is provided by a 1-year record of GCM data. The simulation is conducted for 13 model months, starting from initially low concentrations on 1 December, and the results presented below are from the last 12 months of the simulation (1 January to 31 December). The initial conditions have no influence on the CTM results since 99.6% of the ^{222}Rn initially present on 1 December would have decayed by 1 January, 1 month later.

We assume a standard ^{222}Rn source of 1.0 atoms $cm^{-2}\ s^{-1}$ from unfrozen land surfaces, which is a value intermediate between the global mean flux estimates of 0.75 atoms $cm^{-2}\ s^{-1}$ (Wilkening et al., 1975) and 1.2 atoms $cm^{-2}\ s^{-1}$ (Turekian et al., 1977). This standard source can be modified by soil freezing and by transient changes in surface pressure, as described by Jacob and Prather (1990). Oceanic emissions are neglected because they are too weak to contribute to radonic storms (Broecker et al., 1967; Wilkening and Clements, 1975). Emissions from the Antarctic continent are also neglected; the extremely low ^{222}Rn concentrations observed at South Pole Station (Lockhart, 1964) indicate that the ice cap is not a significant ^{222}Rn source, and the time series of ^{222}Rn concentrations at King George Island show no discernible ^{222}Rn emission from the "dry valleys" at the edge of the continent (Pereira, 1990). The ^{222}Rn emission flux in each CTM gridbox is specified on the basis of land fractions from a $1° \times 1°$ land use map (Matthews, 1983). First- and second-order moments are applied to the source function in order to simulate the emission of ^{222}Rn at the bottom of the gridbox, and resolve the spatial distribution of emissions in coastal gridboxes (Prather et al., 1987; Jacob and Prather, 1990).

Local ^{222}Rn emissions from the island soils at Crozet, Kerguelen, and Amsterdam are not included in the formulation of the ^{222}Rn source. These local emissions are occasionally responsible for observations of radonic storms at the islands, as demonstrated by concurrent measurements of ^{220}Rn, a short-lived isotope of ^{222}Rn (Polian et al., 1986). However, less than 10% of the storms can be explained in this manner (G. Polian, personal communication, 1988).

Numerical diffusion and numerical dispersion are critical concerns when attempting to simulate the distribution of ^{222}Rn over an ocean. The CTM must resolve adequately the sharp boundary between high concentrations over the continent, and low concentrations over an ocean, which is imposed by the spatial distribution of ^{222}Rn emissions and the relatively short half-life of ^{222}Rn. This problem amounts to seeking a non-diffusive and non-dispersive solution for the advection of a step function, a notoriously diffi-

cult exercise for Eulerian transport models (McRae et al., 1982). Prather (1986) examined the transport of a 3-d step function using the second-order moments advection scheme, and found that significant ripples of dispersion (1% of the signal) could extend to 3 gridboxes ahead of the step. Therefore, the islands in the CTM domain should be located at least 4 gridboxes away from the nearest continental source. Crozet is 3 gridboxes south and 4 gridboxes east off the African coast; Kerguelen and Amsterdam are even more remote from continental sources.

3. Model results: comparison with observations

Fig. 2 displays the 1-year time series of simulated ^{222}Rn concentrations at each of the 3 islands. The prominent feature of these time series is the occurrence of sharp peaks rising from a low baseline, simulating radonic storms in a manner that is qualitatively consistent with the observations of Lambert et al. (1970) and Polian et al. (1986). The detail of the observed time series at the islands has not been published, but extensive descriptions of the main features have been presented by Lambert et al. (1970), Polian (1984), and Polian et al. (1986), and will serve here as the basis for evaluating model results. To facilitate the discussion, we define radonic storms in the simulation as occurrences of ^{222}Rn concentrations 3 times in excess of the yearly mean concentration, which is 2.1 pCi/SCM at Crozet, and 1.0 pCi/SCM at both Kerguelen and Amsterdam. With this definition the one-year time series contains 28 separate radonic storm events at Crozet, 27 at Kerguelen, and 12 at Amsterdam. We also define baseline ^{222}Rn concentrations as yearly mean concentrations obtained after removal of all radonic storm events. The values computed in this manner are 1.2 pCi/SCM at Crozet, 0.7 pCi/SCM at Kerguelen, and 0.9 pCi/SCM at Amsterdam. Although the CTM may slightly underestimate the baselines due to the neglect of oceanic ^{222}Rn emissions, the results are in harmony with the observed baselines at the islands (0.2–0.5 pCi/SCM; Polian et al., 1986).

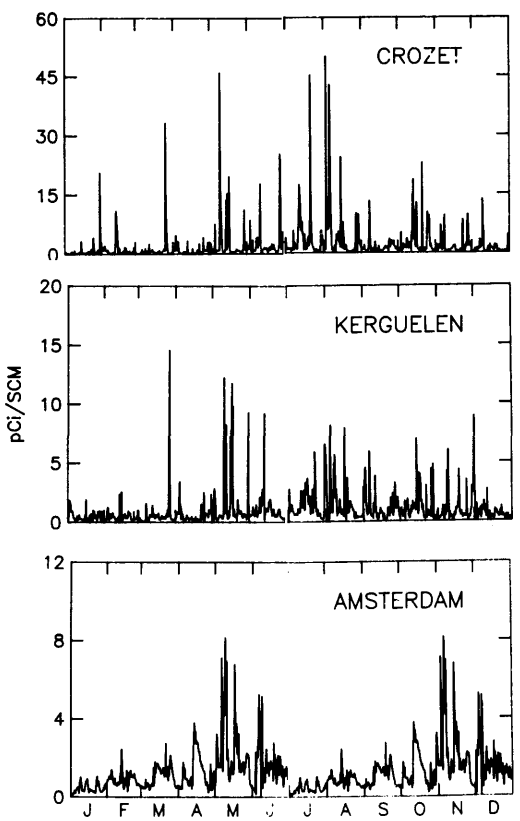

Fig. 2. Time series of simulated ^{222}Rn concentrations at the 3 island sites.

The radonic storms in the CTM vary in intensity and duration. The maximum concentrations achieved in the 1-year simulation are 50 pCi/SCM at Crozet, 15 pCi/SCM at Kerguelen, and 8 pCi/SCM at Amsterdam. The average storm peak is 13 pCi/SCM at Crozet, 5 pCi/SCM at Kerguelen, and 4 pCi/SCM at Amsterdam. By comparison, the observed radonic storms at the islands usually peak at 4–10 pCi/SCM, with exceptional occurrences of 40 pCi/SCM at Crozet and 20 pCi/SCM at Kerguelen and Amsterdam (Polian et al., 1986). Model results are in excellent agreement with these observations. A few radonic storms in the simulation last for only 4 h (one CTM time step), but most persist for 1–2 days, again in harmony with observations (Polian, 1984). The maximum storm duration in the model is 3.5 days at Crozet, 1.8 days at Kerguelen, and 2.8 days at Amsterdam. Only 2 storms at Crozet, and 1 at Amsterdam, persist for more than 2 days.

Observed seasonal trends of ^{222}Rn concentrations at the islands have been reported by Lambert et al. (1970) and by Polian (1984) as monthly average concentrations. Elevated monthly mean concentrations are observed from May to August, corresponding to a maximum frequency of radonic storms during those months. This seasonal trend is well reproduced by the model (Fig. 3), except that the season of elevated concentrations in the model extends to November. The origin of this anomaly will be discussed in Section 5. Model results in Fig. 3 often lie outside the range of interannual variability of the observations, however the discrepancy may not be significant because only 1 year of CTM data was used in the computation of monthly means; the mean concentration for a given month may be determined by the weight of a single radonic storm. In view of this potential for bias, the use of monthly means in the analysis of the simulated time series is of little value except for defining the broad seasonal trend.

A strong 27–28 days periodicity is apparent in the May–October time series of observed ^{222}Rn concentrations at Crozet and Kerguelen (Lambert et al., 1970). We examined the simulated time series for such a periodicity using the maximum entropy method (Press et al., 1986), which provides a particularly good resolution of sharp spectral features; the spectral peaks were independently verified by constructing periodograms (Press et al., 1986). The power spectra of the simulated May–October time series at all 3 islands indicate a strong 25–28 days periodicity (Fig. 4), which matches the periodicity observed

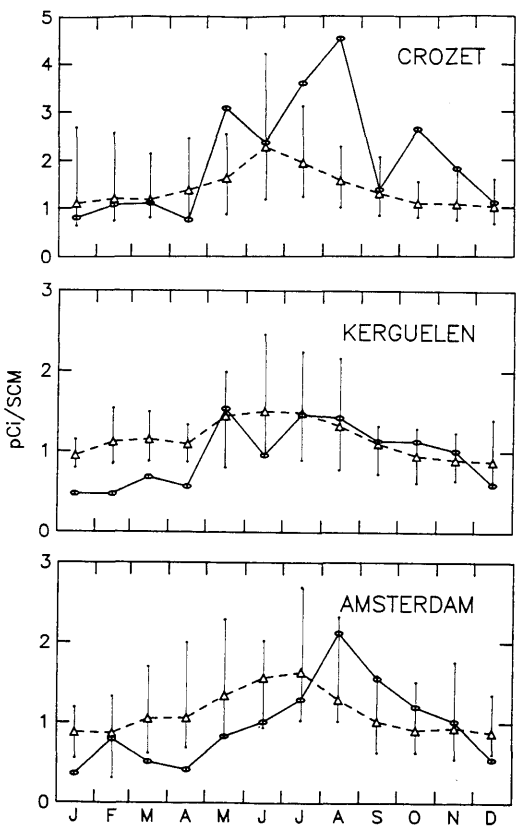

Fig. 3. Monthly mean ^{222}Rn concentrations at the three island sites. Results from the CTM (solid line) are compared to observations (dashed line). The observed monthly means were computed from 17 years of data, 1967–1983 (Polian, 1984). The vertical bars indicate the range of interannual variability of the observations.

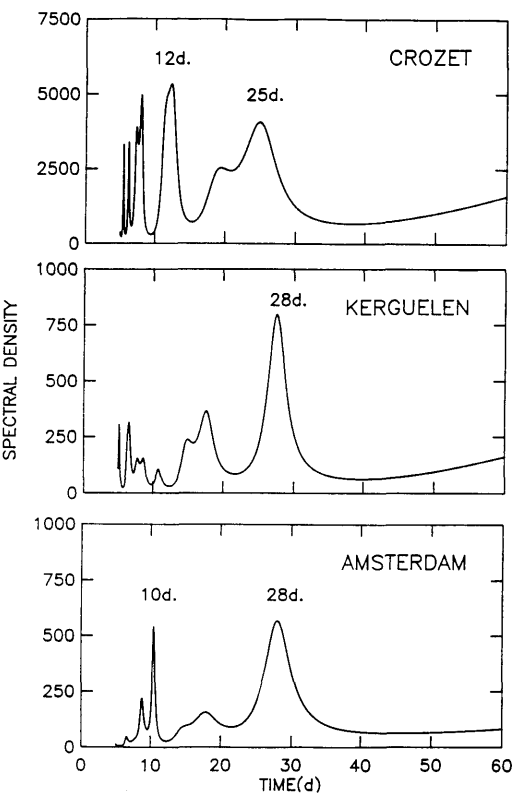

Fig. 4. Power spectra of the simulated ^{222}Rn concentrations (May–October) at the 3 island sites. The power spectra were computed using the maximal entropy method (Press et al., 1986) with 330 poles and 1104 points (6 per day).

by Lambert et al. (1970). A 10–12 days periodicity is also found at Crozet and at Amsterdam, which matches a minor feature in the power spectrum of observations at Crozet (Lambert et al., 1970). The ability of the CTM to simulate the 27–28 days periodicity suggests that this periodicity is due to a meteorological oscillation that is resolved by the GCM. The nature of the oscillation will be discussed in Section 5.

4. Origin of radonic storms in the model

4.1. A case study: 25–27 March

We present here the detailed synoptic analysis of a radonic storm which occurred on 25–27 March of the CTM simulation. The storm appears in the time series at Crozet and Kerguelen as an isolated event under otherwise baseline conditions (Fig. 5). It does not appear in the Amsterdam time series. The contour maps in Fig. 6 document the evolution of ^{222}Rn surface concentrations over the Indian Ocean during the period 23–28 March. The surface concentrations on 23 March are typical of baseline conditions, with values below 1 pCi/SCM over most of the subantarctic Indian Ocean. Concentrations over the tropical Indian Ocean on that day are somewhat higher because of continental influences from southeast Asia. No significant transport from South America to the Indian Ocean is discernible.

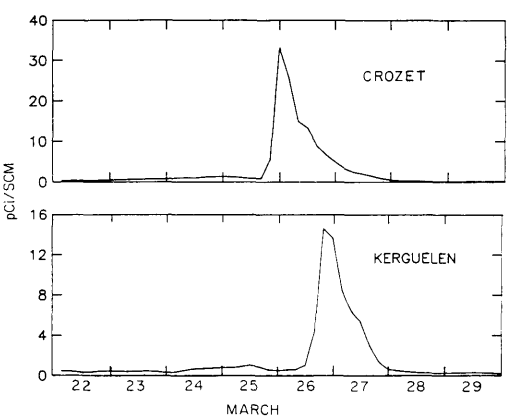

Fig. 5. Time series of ^{222}Rn concentrations at Crozet and Kerguelen for 22–29 March of the CTM simulation.

On 24 March, a NW offshore flow begins to develop off the southern tip of Africa, transporting ^{222}Rn-rich continental air to the subantarctic Indian Ocean. This flow is illustrated in Fig. 6 by the 100 pCi/SCM and 10 pCi/SCM concentration contours, which outline a plume of continental air advected offshore to 1000 km SE off the coast of South Africa. The plume does not reach the islands on 24 March, and the concentrations at Crozet and Kerguelen remain baseline. However the offshore flow persists on 25 March, and the continental plume eventually reaches Crozet on that day at 2000 GMT. The maximum ^{222}Rn concentration at Crozet (33 pCi/SCM) occurs 4 h later, on 26 March at 0000 GMT.

The offshore flow of air from South Africa ceases on 26 March, as indicated in Fig. 6 by the repositioning of the 100 pCi/SCM contour along the edge of the African continent. However a well-defined plume of continental air is still present over the subantarctic Indian Ocean. The plume reaches Kerguelen on 26 March at 1600 GMT, and the maximum concentration at the island (15 pCi/SCM) occurs 4 h later on that day. By that time, the radonic storm at Crozet has already begun to dissipate because of dilution. Further dilution proceeds on 27 March as the plume progressively loses its identity and diffuses throughout the subantarctic Indian Ocean. By 28 March, near-baseline conditions are restored at the islands.

The contour maps of surface concentrations in Fig. 6 suggest that the flow of continental air from southern Africa to Crozet and Kerguelen took place mainly in the boundary layer. This boundary layer mechanism is further demonstrated in Fig. 7 by a cross-section of ^{222}Rn concentrations at 46°S (the latitude of Crozet) on 26 March. The plume of continental air over Crozet is confined to the lower troposphere, with ^{222}Rn concentrations highest at the surface and decreasing sharply with altitude. The ^{222}Rn concentrations in the free troposphere are of order 1 pCi/SCM, typical of background conditions.

The flow pattern during the 25–27 March episode was investigated further by constructing surface pressure maps from the GCM data (Fig. 8). On 24 March we note the combined presence of a high SE of Madagascar, and a low off the tip of South Africa, forming a pressure gradient along the SE edge of the African continent which

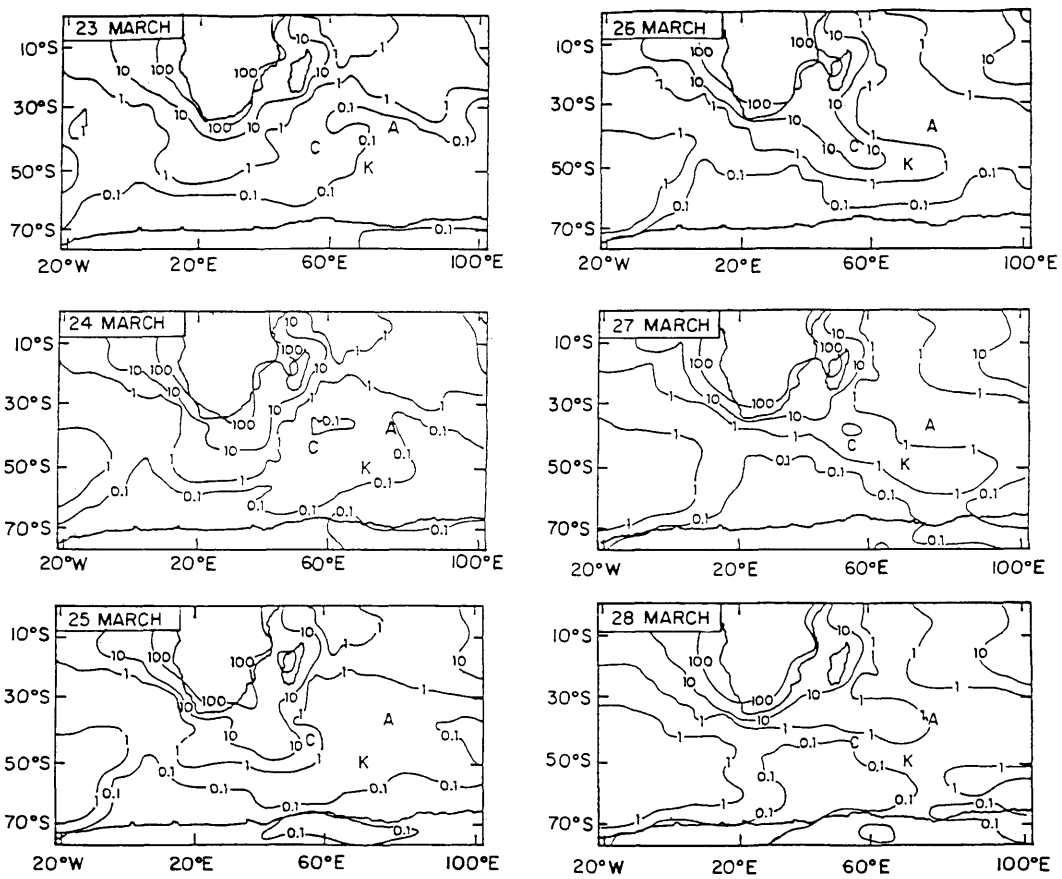

Fig. 6. Surface concentrations of ^{222}Rn for 23–28 March of the CTM simulation. The contours represent 24-h average values (pCi/SCM). The island sites are indicated by their initials, Crozet (C), Kerguelen (K) and Amsterdam (A).

drives the NW flow of continental air towards the subantarctic Indian Ocean. The high in the GCM simulates the Mascarene high, a well-known semi-permanent feature of the circulation over the Indian Ocean (Taljaard and Van Loon, 1984). The low simulates a transient mid-latitudes cyclone which is known as an important element of weather over South Africa (Schulze, 1971). The synoptic pattern of 24 March persists into 25 March, maintaining the offshore flow of continental air; however the pressure gradient along the SE edge of the African continent begins to weaken as the low moves progressively eastwards away from the continent. By 26 March the pressure gradient has vanished, and the flow of continental air to the subantarctic Indian Ocean is suppressed. The plume of continental air advected offshore on 24–25 March is still carried eastward on 26 March under the influence of the Mascarene high, and eventually reaches Kerguelen late on that day. Amsterdam lies under the center of high pressure on 26 March (Fig. 8), and never experiences a radonic storm as the continental air is deflected to the south of the island.

The above analysis demonstrates a clear causal relationship between the establishment of a pressure gradient along the SE edge of the

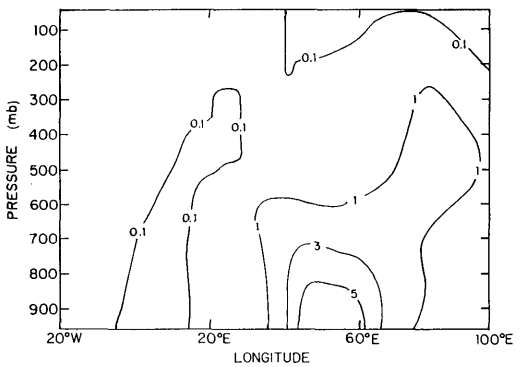

Fig. 7. Concentrations of ^{222}Rn concentrations at 46°S (the latitude of Crozet), on 26 March of the CTM simulation. The contours represent 24-h average values (pCi/SCM).

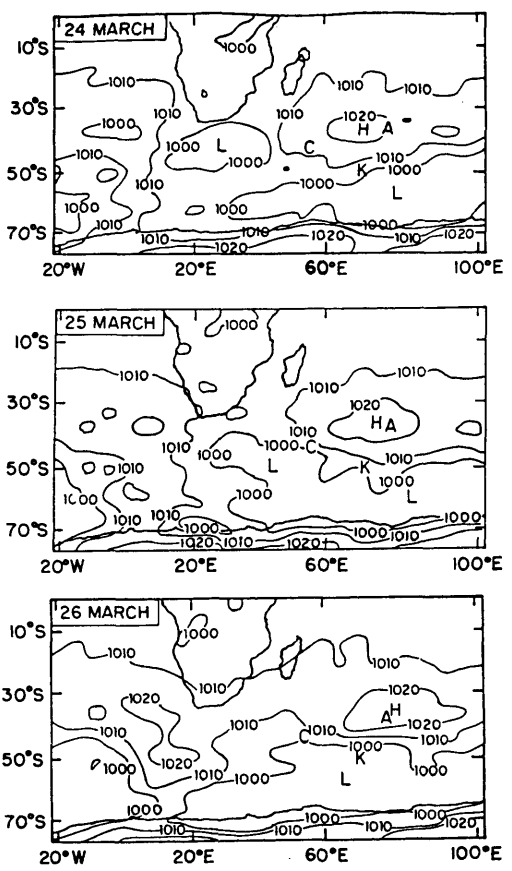

Fig. 8. GCM surface pressure maps (mb) for 24–26 March. The island sites are indicated by their initials, Crozet (C), Kerguelen (K), Amsterdam (A). The contours represent 24-h average values.

African continent on 24–25 March, and the occurrence of a radonic storm at Crozet and Kerguelen a few days later. We can quantify the strength of the offshore flow from the African continent to the subantarctic Indian Ocean by the surface pressure gradient ΔP between the points (25°E, 42°S) and (50°E, 30°S) (Fig. 9). The lower panel of Fig. 9 shows the time series of ΔP for 22–29 March. The maximum in ΔP (24 March at 2000 GMT) should correspond to the most vigorous offshore transport, so that the time lag between the maximum in ΔP and the peak of the radonic storm gives a measure of the oceanic transit time from the continent to the islands. For the March 25–27 storm we deduce transit times of 1.2 days for Crozet and 2.0 days for Kerguelen.

4.2. Generalization

We now attempt to generalize our analysis of the 25–27 March storm to the other storms in the CTM simulation. The contribution of southern Africa to the radonic storms was determined by conducting a separate 1-year CTM simulation with identical meteorology but where southern Africa (the fraction of the continent south of the equator) was the only source of ^{222}Rn. This simulation was conducted on a window of the global CTM grid (Prather et al., 1987) in order to limit computational cost. The window extended

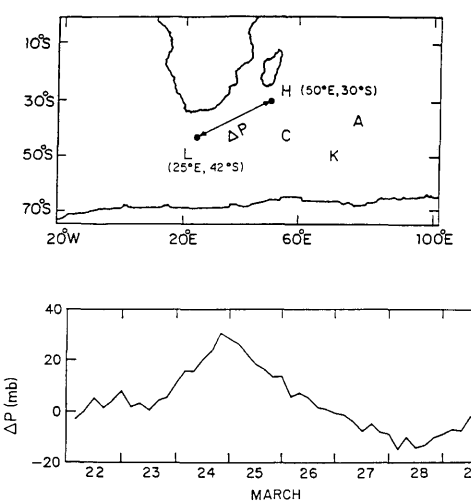

Fig. 9. Upper panel: definition of the pressure difference ΔP. Lower panel: time series of ΔP for 22–29 March of the CTM simulation.

from 20°W to 95°E, and from the equator to 72°S. Low baseline concentrations (0.15 pCi/SCM) were assumed as boundary conditions along the edges of the window. Such low concentrations are clearly unrealistic for the northern edge, particularly the portion which intersects the African continent, but in this manner the window simulation is guaranteed to provide a conservative estimate of the southern Africa contribution to the radonic storms.

We find that the CTM window simulation with southern Africa as the only source replicates closely all the individual radonic storms of the global simulation, except for one relatively weak event on 10 June where transport from South America may be implicated. The average concentrations during radonic storms are underestimated by only 1.3 pCi/SCM at Crozet, 0.9 pCi/SCM at Kerguelen, and 0.8 pCi/SCM at Amsterdam. These underestimates are of the order of the baseline, and are insignificant considering the uncertainty introduced by the boundary conditions. We conclude that the radonic storms in the CTM originate almost exclusively from southern Africa.

Comparison of boundary layer versus free troposphere ^{222}Rn concentrations over the islands during radonic storms provides a diagnostic of whether the transport of continental air took place in the boundary layer or in the free troposphere. We show in Table 1 the averages of simulated concentrations at the surface and at 500 mb, under both baseline and storm conditions. Under baseline conditions the ^{222}Rn concentrations are higher aloft than at the surface, consistent with observed vertical profiles over Kerguelen (Polian et al., 1986) and consistent also with typical observations over the oceans (Lenschow et al., 1988; Kritz et al., 1990). Under radonic storm conditions the vertical gradients of ^{222}Rn concentrations at Crozet and at Kerguelen are reversed compared to baseline conditions, i.e., concentrations are higher at the surface than in the free troposphere. The reversal of the gradient is a clear indication that boundary layer advection of continental air is responsible for the occurrence of radonic storms. The concentrations at 500 mb are somewhat higher under radonic storm conditions than under baseline conditions, for two reasons: (1) the boundary layer plume of continental air diffuses upwards as it is advected towards the islands; (2) the synoptic pattern favoring the offshore flow of continental air in the boundary layer also favors a similar flow in

Table 1. *Simulated ^{222}Rn concentrations (pCi/SCM) at the surface and at 500 mb*

	Baseline		Storm	
	surface	500 mb	surface	500 mb
Crozet	1.2	2.7	13.3	4.5
Kerguelen	0.7	2.0	5.3	3.2
Amsterdam	0.9	2.6	4.3	4.5

Values are yearly mean concentrations. "Baseline" and "storm" conditions are defined in the text.

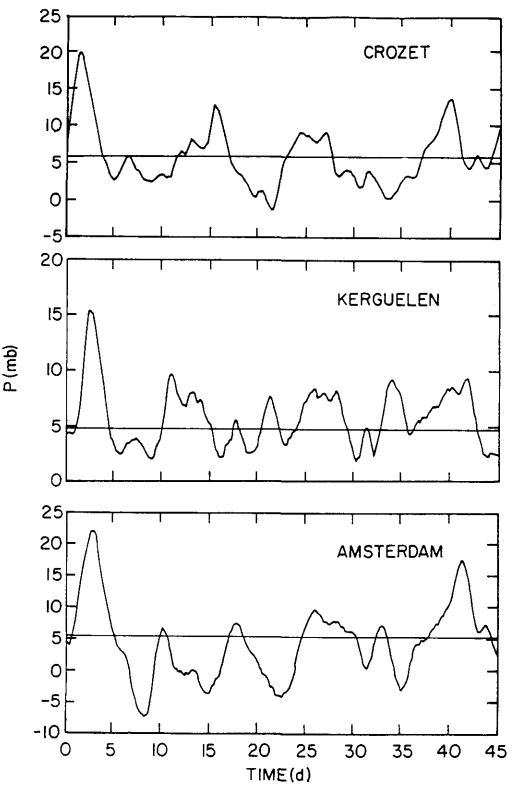

Fig. 10. Mean value of ΔP versus time lag before a radonic storm at the three island sites. The analysis was restricted to the May–October interval. The May–October mean value of ΔP is shown as the horizontal line on each graph.

the free troposphere. By the time the radonic storms reach Amsterdam extensive horizontal and vertical diffusion of the boundary layer plume has had time to proceed, and the ^{222}Rn concentrations at the surface and 500 mb are of similar magnitude.

The correlation between radonic storms and the establishment of the pressure gradient ΔP off the SE edge of the African continent can also be generalized. We show in Fig. 10 the mean values of ΔP at the 3 islands as a function of time lag before the occurrence of a radonic storm. Unusually high values of ΔP are found in the days immediately preceding a storm, confirming the causal relationship between ΔP and the occurrence of radonic storms. The peak value of ΔP occurs on average 1.5 days before a storm at Crozet, and 2.8 days before a storm at Kerguelen and Amsterdam; as discussed above, these time lags provide an estimate of the mean transit time of ^{222}Rn from the continent to the islands. By comparison, Polian et al. (1986) reported average transit time of 1.7 days for the observed storms at Crozet, 2.5 days at Kerguelen, and 3.0 days at Amsterdam, on the basis of estimated wind speeds. Model results are in excellent agreement with these estimates.

5. Discussion

5.1. Seasonality and periodicity of radonic storms

The main cause of radonic storms in the CTM is the establishment of a strong pressure gradient ΔP along the SE edge of the African continent. Since the CTM succeeds in simulating both the seasonality and the periodicity of the radonic storms, we conclude that both of these features must originate from properties of ΔP. We examine here in more detail the behavior of ΔP, and of the contributing "high" (50°E, 30°S) and "low" (25°E, 42°S), using both GCM results and meteorological observations. The observations consist of twice-daily measurements of surface pressure at the locations of the high and the low. A continuous 5-year record of observations for 1975–1979 was retrieved from archives at the National Center for Atmospheric Research (National Center for Atmospheric Research, 1987).

The seasonal patterns of ΔP and of the contributing high and low are shown in Figure 11, for both GCM and observations. Elevated values of ΔP are found in the GCM from May to November, with a July anomaly. This seasonality of ΔP matches the seasonality of radonic storms in the CTM, except that storms still occur in July despite the anomaly in ΔP. Separate inspection of the two July storms at Crozet indicates that on those two occasions the pressure gradient along the SE coast of Africa was displaced from the usual location measured by ΔP. The seasonal trend of ΔP in the observations is similar to that in the GCM, with elevated values from June to September which match the observed seasonality of radonic storms. The high October and November values of ΔP in the GCM are anomalous, and

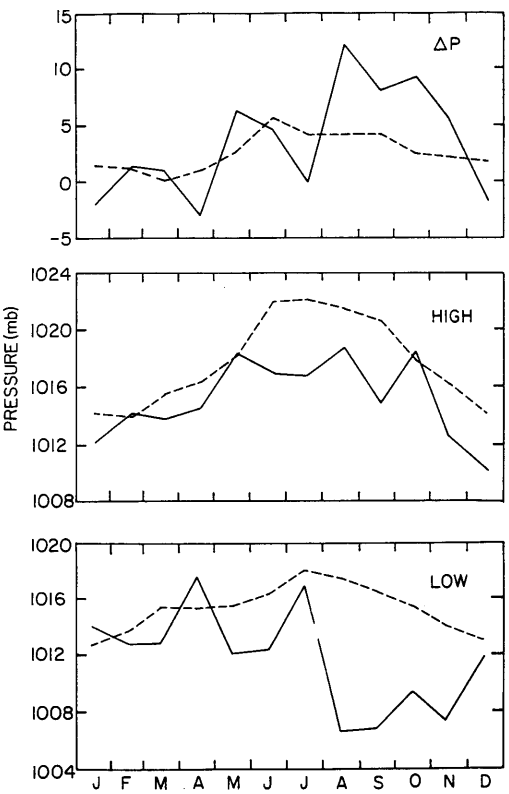

Fig. 11. Monthly mean values of ΔP and of the contributing high: (50°S, 30°S) and low (25°E, 42°S); GCM results from a one-year run (solid lines) are compared to observations for 1975–1979 (dashed lines).

probably explain why excessive ^{222}Rn concentrations are predicted during those two months (Fig. 3).

The seasonal trend of ΔP in the GCM and in the observations is imposed by the seasonal trend of the high (Fig. 11); the seasonal trend of the low tends to be of opposite phase. The seasonal frequency of radonic storms at the islands is therefore controlled by the strength of the Mascarene high (of which the high entering in the formulation of ΔP constitutes a westward extension). The climatology of the Mascarene high over the Indian Ocean has been discussed in detail by Taljaard and Van Loon (1984). From May to October, the high is semi-permanent and nearly stationary SE of Madagascar; in other months, it is weaker and displaced eastwards. This seasonal pattern of the Mascarene high matches closely the observed seasonal pattern of radonic storms.

The presence of the high does not however suffice to produce elevated ^{222}Rn concentrations at the islands. In the CTM the baseline ^{222}Rn concentrations during May–October are only slightly higher than in the rest of the year, and radonic storms (although more frequent) still occur only sporadically. The establishment of a strong pressure gradient ΔP requires in addition the presence of the transient mid-latitudes low. Since the variance of the low is considerably greater than that of the high, the high-frequency fluctuations in ΔP, which are at the origin of the radonic storms, tend to be largely controlled by fluctuations of the low. In the GCM, ΔP is strongly correlated with the low ($r = -0.93$) but only weakly correlated with the high ($r = 0.40$); similarly, in the 5 years of surface pressure observations, ΔP is strongly correlated with the low ($r = -0.79$ to -0.86 depending on the year) and only weakly correlated with the high ($r = 0.30$ to 0.49). We conclude that the occurrences of radonic storms should follow closely from fluctuations in the low, and therefore that the periodicity of the storms should originate from an oscillation of the low.

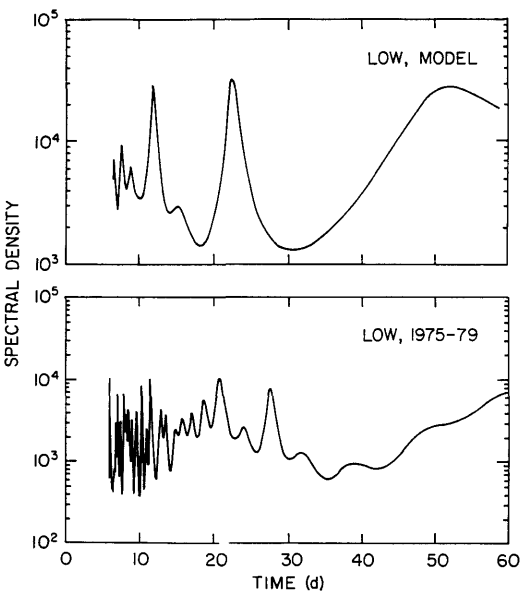

Fig. 12. Power spectra of the low (25°E, 42°S) during May–October, in the GCM and in the 1975–1979 observations. The power spectra were computed using the maximal entropy method (Press et al., 1986) with 430 poles and 1440 points for the observations, and with 330 poles and 1104 points in the model. The number of poles was chosen so that the ratio of the number of points to the number of poles was the same as in Fig. 4.

Power spectra of the low are shown in Fig. 12, for both the GCM and the 1975–1979 observations; the analysis was confined to the interval May–October to allow comparison with the ^{222}Rn results. We find prominent periodicities at 23 days in the GCM, and at 27 days in the observations, which match fairly well the periodicities of the radonic storms. Inspection of individual years from the 1975–1979 database indicates that the periodicity is present in all years, though the location of the peak varies from 23 days (1975) to 28 days (1978). If the GCM is indeed able to reproduce the meteorological oscillation at the origin of the radonic storms, then speculations regarding the origin of the oscillation are severely restricted. In particular, oscillatory phenomena stemming from tides or solar radiation can be excluded since they are not resolved by the GCM. Further examination of the GCM oscillation would be of interest but lies beyond the scope of this paper.

5.2. Export of air from South Africa to southern mid-latitudes

The radonic storms offer evidence for rapid transport of continental air from South Africa to southern mid-latitudes. A simple airshed analysis

Table 2. *Simulated monthly mean budget of ^{222}Rn in the South Africa airshed*

	January		August	
	surface–720 mb	720–70 mb	surface–720 mb	720–70 mb
Emission	+95	0	+97	0
flux at 28°S (N boundary)	+14	+20	+52	+11
flux at 40°S (S boundary)	−8	−8	−28	−29
flux at 12°30′E (W boundary)	−11	+17	−5	+9
flux at 42°30′E (E boundary)	−5	−43	−18	−37
total flux to Indian Ocean[a]	−13	−51	−46	−66

Units are 10^{-2} Ci s^{-1}. Airshed boundaries are shown in Fig. 1. A positive flux indicates a net flow of ^{222}Rn into the airshed.The total area of the airshed is 3.68 10^{12} m^2.

[a] Defined as the sum of the fluxes at 40°S and at 42°30′E (S and E boundaries).

based on the CTM results allows an estimate of the mass fluxes involved. For the purpose of this analysis, we define a South Africa airshed as the atmospheric column with boundaries (12°30′E, 42°30′E, 28°S, 40°S), corresponding roughly to the political boundaries of South Africa and including the immediately adjacent waters (Fig. 1). Table 2 shows the monthly mean ^{222}Rn fluxes through the boundaries of the airshed, for January and August. The fluxes are segregated between boundary layer (surface–720 mb) and free troposphere (720–70 mb); vertical transport of ^{222}Rn across the 70 mb surface is negligible. The main sources of ^{222}Rn to the airshed are local emissions (60–75% of the total source) and southward transport across the 28°S boundary.

Inspection of the fluxes in Table 2 indicates that South Africa is rapidly ventilated by eastward and southward transport to the Indian Ocean. The sum of the eastward flux at 42°30′E and of the southward flux at 40°S corresponds to about 50% of the total ^{222}Rn input to the airshed in January, and 70% of that input in August. Most of the transport takes place in the free troposphere; the contribution from boundary layer advection (as would be associated with radonic storms) amounts to only 20% of the total flux in January and 40% in August. The boundary layer flux from South Africa to the Indian Ocean is 4 times higher in August than in January because of the stronger Mascarene high; the free troposphere flux increases by only a small factor (30%) between January and August.

Our results suggest that rapid export of air from South Africa to the Indian Ocean could provide a major input of pollution at southern mid-latitudes. Some of this pollution reaches the subantarctic Indian Ocean in the form of well-defined boundary layer plumes of continental air, as identified by radonic storms at the ocean surface. However, we find that most of the pollutant transport takes place in the free troposphere following deep convection over the continent. The boundary layer advection mechanism associated with radonic storms should thus account for only a minor fraction of the total continental air advected over the subantarctic Indian Ocean.

6. Acknowledgements

We thank Roy Jenne and Gregg Walters from the National Center for Atmospheric Research for providing support using the NCAR database, and Aratha Johnson for her help with the figures. We acknowledge useful discussions with Inez Fung, Gary Russell, Tony del Genio and Jean Lerner from GISS. We also acknowledge computing support from NCAR (the National Center for Atmospheric Research is sponsored by the National Science Foundation). This work was supported by the National Science Foundation (grants ATM87-19224 and ATM84-13153) and by the National Aeronautics and Space Administration (grant NASA-NAG5-719).

REFERENCES

Andreae, M. O., Berresheim, H., Andreae, T. W., Kritz, M. A., Bates, T. S. and Merrill, J. T. 1988. Vertical distribution of dimethylsulfide, sulfur dioxide, aerosol ions, and radon over the northeast pacific ocean. *J. Atmos. Chem. 6*, 149–173.

Broecker, W. S., Li, Y. H. and Cromwell, J. 1967. Radium-226 and radon-222: concentrations in Atlantic and Pacific Oceans. *Science 158*, 1307–1310.

Cadet, D. 1983. The monsoon over the Indian Ocean during summer 1975. Part II: break and active monsoons. *Mon. Weath. Rev. 111*, 95–108.

Carlson, T. N. and Prospero, J. M. 1972. The large scale movement of Saharan air outbreaks over the equatorial North Atlantic. *J. App. Meteor. 11*, 283–297.

Fishman, J., Watson, E. C. and Larsen, J. C. 1989. The distribution of total ozone, and tropospheric ozone at low latitudes deduced from satellite data sets. *Quadrennial Ozone Symposium* (August 1988), University of Gottingen, Federal Republic of Germany.

Fraser, P. J., Hyson, P., Rasmussen, R. A., Crawford, A. J. and Khalil, M. A. K. 1986. Methane, carbon monoxide and methyl chloroform in the southern hemisphere. *J. Atmos. Chem. 4*, 3-42.

Fuggle, R. F. and Rabie, M. A. 1983. Environmental Concerns in South Africa: *Technical and Legal Perspectives* (Eds. Fuggle, R. F. and Rabie, M. A.) Juta, Cape Town, 283–301.

Fung, I., Prentice, E., Matthews, E., Lerner, J. and Russell, G. 1983. Three-dimensional tracer model study of atmospheric CO_2: response to seasonal exchanges with the terrestrial biosphere. *J. Geophys. Res. 88*, 1281–1294.

Gesell, T. F. 1983. Background atmospheric ^{222}Rn concentrations outdoors and indoors: a review. *Health Phys. 45*, 289–302.

Hansen, J., Russell, G., Rind, D., Stone, P., Lacis, A., Lebedeff, S., Ruedy, R. and Travis, L. 1983. Efficient three-dimensional global models for climate studies: models I and II. *Mon. Weath. Rev. 111*, 609–662.

Jacob, D. J., Prather, M. J., Wofsy, S. C. and McElroy, M. B. 1987. Atmospheric distribution of ^{85}Kr simulated with a general circulation model. *J. Geophys. Res. 92*, 6614–6626.

Jacob, D. J. and Prather, M. J. 1990. Radon-222 as a test of convective transport in a general circulation model. *Tellus 42B*, 118–134.

Kidson, J. W. 1986. Index cycles in the southern hemisphere during the global weather experiment. *Mon. Weath. Rev. 114*, 1654–1663.

Krishnamurti, T. N. and Bhalme, H. N. 1976. Oscillations in a monsoon system. Part I. Observational aspects. *J. Atmos. Sci. 33*, 1937–1954.

Kritz, M. A., Leroulley, J. C. and Danielsen, E. F. 1990. The China Clipper—Fast advective transport of radon rich air from the Asian boundary layer to the upper troposphere near California. *Tellus 42B*, 46–61.

Lambert, G., Polian, G. and Taupin, D. 1970. Existence of periodicity in radon concentrations and in the large-scale circulation at latitudes between 40° and 70° South. *J. Geophys. Res. 75*, 2341–2345.

Lambert, G., Polian, G., Sanak, J., Ardouin, B., Buisson, A., Jegou, A. and Leroulley, J. C. 1982. Cycle du radon et de ses descendants: application à l'étude des échanges troposphère-stratosphère. *Ann. Geophys. 38*, 497–531.

Lenschow, D. H., Paluch, I. R., Bandy, A. R., Pearson, R., Jr., Kawa, S. R., Weaver, C. J., Huebert, B. J., Kay, J. G., Thornton, D. C. and Driedger III. 1988. Dynamics and chemistry of marine stratocumulus (DYCOMS) experiment. *Bull. Amer. Met. Soc. 69*, 1058–1067.

Leovy, C. B. and Webster, P. J. 1976. Stratospheric long waves: comparison of thermal structure in the northern and the southern hemispheres. *J. Atmos. Sci. 33*, 1624–1638.

Lockhart, L. B., Jr. 1964. Radioactivity of the radon-222 and radon-220 series in the air at ground level. In: *The Natural Environment* (eds. Adams, J. A. S. and Lowder, W. M.). University of Chicago Press, Chicago, 331–344.

McRae, G. J., Goodin, W. R. and Seinfeld, J. H. 1982. Numerical solution of the atmospheric diffusion equation for chemically reacting flows. *J. Comput. Phys. 45*, 1-42.

Matthews, E. 1983. Global vegetation and land use: new high-resolution data bases for climate studies. *J. Climat. Appl. Meteor. 22*, 272–287.

Merrill, T. J., Bleck, R. and Lixion, A. 1985. Modeling atmospheric transport to the Marshall islands. *J. Geophys. Res. 90*, 12927–12936.

National Center for Atmospheric Research. 1987. Daily grid point analysis data. Australian. Available from National Center for Atmospheric Research, Data Support Section, Boulder, Colorado 80307, USA.

Newell, R. E, Shipley, S. T., Connors, V. S. and Reichle, H. G. 1988. Regional studies of potential carbon monoxide sources based on space shuttle and aircraft measurements. *J. Atmos. Chem. 6*, 61–81.

Pereira, E. B. 1990. Radon-222 time series measurements in the Antarctic peninsula (1986–1987). *Tellus 42B*, 39–45.

Polian, G. 1984. *Les transports hémisphériques dans l'hémisphère sud, et le bilan global du radon 222.* Ph.D. Thesis, Univ. P. M. Curie, Paris 6, France.

Polian, G., Lambert, G., Ardouin, B. and Jegou, A. 1986. Long-range transport of continental radon in subantarctic and antarctic areas. *Tellus 38B*, 178–189.

Prather, M. J. 1986. Numerical advection by conservation of second order moments. *J. Geophys. Res. 91*, 6671–6681.

Prather, M. J., McElroy, M. B., Wofsy, S. C., Russell, G. and Rind, D. 1987. Chemistry of the global troposphere: fluorocarbons as tracers of air motion. *J. Geophys. Res. 92*, 6579–6613.

Press, W. H., Flannery, P. F., Teukosly, S. A. and Vetterling, W. T. 1986. *Numerical recipes*. Cambridge: Cambridge University Press, pp. 430–436.

Schulze, B. R. 1971. South Africa. In: *World survey of climatology* (ed. J. F. Griffiths). Amsterdam: Elsevier. *10*, 501–555.

Taljaard, J. J. and Van Loon, H. 1984. Climate of the Indian Ocean South of 35°S. In: *World survey of climatology* (ed. J. F. Griffiths). Amsterdam: Elsevier. *15*, 505–591.

Turekian, K. K., Nozaki, Y. and Benninger, L. K. 1977. Geochemistry of atmospheric radon and radon products. *Ann. Rev. Earth Planet. Sci. 5*, 227–255.

Uematsu, M., Duce, R. A., Prospero, J. M., Chen, L., Merrill, J. T. and McDonald, R. L. 1983. Transport of mineral aerosol from Asia over the North Pacific ocean. *J. Geophys. Res. 88*, 5343–5352.

Whelpdale, D. M., Eliassen, A., Galloway, J. N., Dovland, H. and Miller, J. M. 1988. The transatlantic transport of sulfur. *Tellus 40B*, 1–15.

Wilkening, M. H. and Clements, W. E. 1975. Radon 222 from the ocean surface. *J. Geophys. Res. 80*, 3828–3830.

Wilkening, M. H., Clements, W. E. and Stanley, D. 1975. Radon 222 flux measurements in widely separated regions. In: *The natural radiation environment (II)* (eds. Adams, J. A. S., Lowder, W. M. and Gesell, T. F.). USERDA Conf. 720805, 717–730.